Light-Driven Electron Transfer through a Water−Oil Interface by a Shuttle Photosensitizer: Photoinduced Electron Transfer from Tributylamine to $Fe(CN)_6^{3-}$ Using Ethyl Eosin as a Mediator in a Water-in-Oil Microemulsion System

Itamar Willner* and Ernesto Joselevich

Institute of Chemistry and The Farkas Center for Light-Induced Processes, The Hebrew University of Jerusalem, Jerusalem 91904, Israel

Received: March 23, 1999; In Final Form: July 1, 1999

Photoinduced electron transfer between water−oil phases is accomplished in a water-in-oil microemulsion system using a "shuttle photosensitizer" as an electron transporter. The system consists of a water-in-oil microemulsion in which ethyl eosin, $^1EtEo^-$, acts as a photosensitizer, $Fe(CN)_6^{3-}$ as an electron acceptor, and tributylamine, Bu_3N, as an electron donor. The hydrophilic photosensitizer and electron acceptor are solubilized in the aqueous microdroplets of the water-in-oil microemulsion, whereas the hydrophobic electron donor is present in the continuous oil phase. Photoinduced oxidative electron-transfer quenching in the water phase, $k_q = 1.7 \times 10^5\ s^{-1}$, results in the oxidized photosensitizer, $^2EtEo^\bullet$, and $Fe(CN)_6^{4-}$. The hydrophobic oxidized photosensitizer is extracted to the continuous oil phase, resulting in the phase separation of the photogenerated redox species, and the stabilization of the products against back electron transfer, $k_{rec} = 7.1 \times 10^2\ s^{-1}$. The stabilization of the redox species against back electron transfer enables the reduction of the oxidized photosensitizer, $^2EtEo^\bullet$, by Bu_3N in the oil phase, $k_{red} = 1.1 \times 10^6\ M^{-1}\cdot s^{-1}$. The latter process regenerates the hydrophilic photosensitizer, $^1EoEt^-$, that is transported back to the water microdroplets, a process leading to the electron transfer across the water−oil boundary by the shuttle photosensitizer. The photosensitized reduction of $Fe(CN)_6^{3-}$ by Bu_3N, in the water-in-oil microemulsion system, proceeds with a quantum yield of $\phi = 0.04$. The mechanism involved in the photoinduced electron transfer between the water−oil phases is elucidated by time-resolved laser flash photolysis experiments and steady-state irradiation. A detailed mathematical model, assuming a Poisson distribution of the quencher in the water droplets, is formulated. This accounts for the different processes involved in the electron transfer in the microheterogeneous system.

Introduction

Reverse micelles and water-in-oil microemulsions have been extensively applied as organized microheterogeneous environments for controlling photochemical transformations, and, particularly, photoinduced electron transfer.[1,2] Water-in-oil microemulsions were used as microreactors for the preparation of semiconductor nanoclusters[3] and for the effective photosensitization of the resulting semiconducting particles.[4] Charge separation of photogenerated electron-transfer products has been accomplished in water-in-oil microemulsions by controlling the hydrophobic and hydrophilic properties of the redox species.[5] Also, enzymes were solubilized in reverse micelles,[6] and enhanced photoenzymatic activity was observed in this microheterogeneous system.[7] In general, photosensitizer−donor/acceptor couples cosolubilized in the water pools of a water-in-oil microemulsion yield enhanced forward electron-transfer quenching and rapid recombination of the photogenerated redox species due to the structural confinement of the reactants/products in the aqueous droplets. Charge separation in microheterogeneous water-in-oil microemulsions can be accomplished, however, if the photochemically driven electron transfer induces hydrophobic character in one of the redox products, resulting in the phase separation of the oxidized/reduced species in the water−oil phases, respectively. In a previous report,[8] four different configurations of photosensitizer−electron acceptor/donor assemblies in water-in-oil microemulsions were suggested to lead to charge separation by the photochemical electron-transfer-induced hydrophobicity principle, using oxidative or reductive electron-transfer quenching routes. In a detailed photophysical study,[8] we reported on the photochemical reduction of $Fe(CN)_6^{3-}$ by ethyl eosin, $EoEt^-$ (**1**), in a water-in-oil microemulsion, using the electron-transfer-induced hydrophobicity principle, Scheme 1. The photosensitizer is negatively charged, and hence confined together with the electron acceptor to the water microdroplets. Photoinduced electron transfer yields the neutral oxidized photosensitizer that is being extracted to the oil phase, leading to charge separation and stabilization of the redox products against back electron transfer.

In the present paper we extend the concept of the electron-transfer-induced hydrophobicity principle to tailor microheterogeneous water-in-oil microemulsion systems where light-driven electron transfer across the water−oil boundary is stimulated by a "shuttle photosensitizer", Scheme 2. The photogenerated oxidized chromophore is oxidized by an electron donor confined to the oil phase. This process regenerates the ground-state photosensitizer that is re-extracted to the water microdroplets. That is, photoinduced electron transfer from the electron acceptor confined to the aqueous phase to the donor solubilized in the oil phase proceeds by the photosensitizer shuttle. Specifically, we address the photoinduced reduction of

10.1021/jp990997w CCC: $18.00
Published on Web 09/08/1999

SCHEME 1: Kinetic Scheme for the Photoreaction of $EoEt^-$ with $Fe(CN)_6^{3-}$ in a Reverse Micelle Containing *n* $Fe(CN)_6^{3-}$ Quencher Units Using the Electron-Transfer-Induced Hydrophobicity Concept

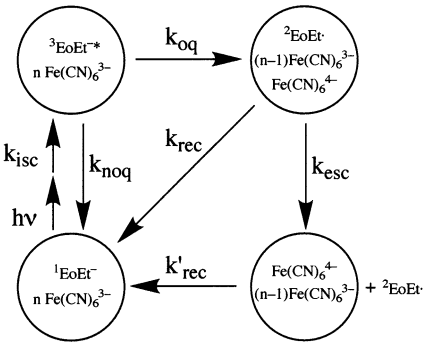

SCHEME 2: Light-Driven Electron Transfer across the Water−Oil Boundary by a Shuttle Photosensitizer

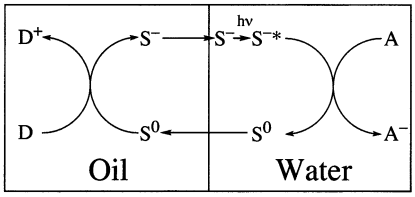

$Fe(CN)_6^{3-}$ by tributylamine, confined to the continuous oil phase, using ethyl eosin (**1**) as a shuttle photosensitizer.

Experimental Section

Eosin (disodium salt), Eo^{2-}, ethyl eosin (potassium salt), $EoEt^-$ (purchased from Aldrich), and potassium ferricyanide, $Fe(CN)_6^{3-}$ (from BDH), were used without further purification. Bis(2-ethylhexyl) sulfosuccinate sodium salt, AOT (from Aldrich), was dried as follows: 25 g of AOT was dissolved in 125 mL of toluene. The toluene-water azeotrope was distilled off (85−90 °C) followed by distillation of most of the toluene. The remaining solvent was removed in vacuo, and the AOT was kept in a desiccator overnight. Heptane (analytical grade BDH) and triply distilled water were used for the preparation of the reverse micelles.

Steady-state absorption spectra were recorded with a Uvikon 860 (Kontron) spectrophotometer. Laser flash photolysis experiments were carried out with the second harmonic generation (532 nm) of a Nd:YAG laser (Laser Photonics Model 34-10) coupled to a detection system (Applied Photophysics K-347) that included a pulsed Xe arc lamp (ORC) as the analytical light source, a monochromator (Applied Photophysics f/3.4) and a photomultiplier (Hamamatsu) linked to a digital oscilloscope (Tektronix 2430A), and an IBM-compatible computer for data storage. The laser pulses had 9 ns width, 20 mJ energy, and 1 Hz frequency, and the beam path through the sample was 0.4 cm. For the kinetic measurements at $\lambda = 460$, 510, and 600 nm, a cutoff filter of $\lambda = 435$ nm was placed between the analytical light source and the sample (optical path $d = 1$ cm), and 64 after-pulse traces were averaged for each measurement. After these low-energy pulses, less than 5% decrease in the absorption of Eo^{2-} and $EoEt^-$, due to irreversible degradation, was detected. For the recording of the transient absorption spectra, a cutoff filter of $\lambda = 360$ nm was used and four traces were averaged for each wavelength from 370 to 620 nm, at intervals of 10 nm. For the millisecond time scale measurements, the Xe arc lamp was used in a continuous mode. Samples (1.2 cm^3) were degassed by argon bubbling for 15 min. Temperature was kept constant at 25 °C throughout all the experiments. Steady-state irradiations were performed with a 150 W Xe arc lamp (Oriel).

SCHEME 3: Kinetic Scheme for the Photochemical Reaction in the Reverse Micellar System Consisting of $Fe(CN)_6^{3-}$/EoEt−/Bu_3N.

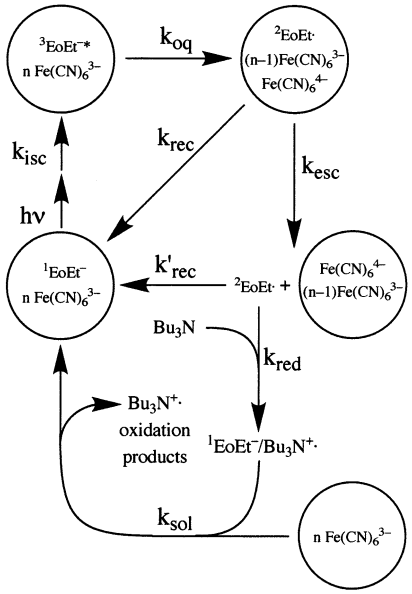

The reverse micelles containing Eo^{2-} and $Fe(CN)_6^{3-}$ were prepared by adding to a 0.05 M AOT solution in heptane (25 mL) the following ingredients: 25 μL of an aqueous 10^{-2} M Eo^{2-} solution, the required amount of an aqueous 5×10^{-2} M $Fe(CN)_6^{3-}$ solution, and the additional volume of water necessary to adjust the water-to-surfactant molar ratio *w* to the desired value ($w = 30$). The mixtures were vigorously stirred until they became completely clear. Sometimes, the process of formation of the clear microemulsion was accelerated by gentle heating, followed by gradual decreasing of the temperature to 25 °C. All samples were kept at 25 °C for at least 30 min before the experiments. The reverse micelles containing $EoEt^-$ and $Fe(CN)_6^{3-}$ were prepared in a similar way, except that the $EoEt^-$ was not introduced as an aqueous solution, due to its lower solubility. Instead, 25 μL of a 10^{-2} M $EoEt^-$ solution in methanol was introduced into the dry beaker, and after evaporation of the methanol, the rest of the ingredients were added. Although the reverse-micellar systems were stable for weeks, the measurements were carried out within 2 days after preparation of the microemulsions. The dye concentration in all the systems was 1×10^{-5} M, whereas the $Fe(CN)_6^{3-}$ concentration varied from 0 to 2.5×10^{-4} M. For steady-state irradiation, tributylamine, Bu_3N, was injected into the water-in-oil microemulsion systems.

Results and Discussion

The photophysics of xanthene dyes and, specifically, eosin derivatives was extensively studied.[9−11] Xanthene dyes were employed as photosensitizers to induce electron transfer[12] and for the photosensitization of semiconductors,[13,14] for the spectral sensitization of photographic emulsions,[15] and for the organization of semisynthetic photoenzymes.[16]

The kinetic scheme for the photoinduced electron transfer in the composite water-in-oil microemulsion consisting of $Fe(CN)_6^{3-}$/$EoEt^-$/Bu_3N is displayed in Scheme 3. It includes the oxidative quenching of $^3EoEt^{-*}$ by $Fe(CN)_6^{3-}$ in the water droplet, to yield the neutral hydrophobic product, $^2EoEt^{\bullet}$. Phase

transfer of the oxidized product, ^{2}EoEt$^\bullet$, to the oil phase competes with the intradroplet recombination of the redox products. The phase-separated products are anticipated to be stabilized against back electron transfer (k'_{rec} is low). This allows the secondary oxidation of Bu_3N by ^{2}EoEt$^\bullet$, acting as an electron-transfer shuttle between the two phases. The oxidation of Bu_3N by ^{2}EoEt$^\bullet$ regenerates the photosensitizer in the aqueous droplet. As the primary photogenerated redox products are separated by means of the two phases and are substantially stabilized against back electron transfer, one can analyze the elementary kinetic steps involved in the electron transfer across the water−oil boundary by the shuttle photosensitizer by two separate mechanistic blocks: (i) the primary electron-transfer events in the water microdroplets and the subsequent phase separation of the redox species by the electron-transfer-induced hydrophobicity principle; (ii) the secondary oxidation of the electron donor (Bu_3N) confined to the oil phase by the photosensitizer shuttle, and the regeneration of the ground-state photosensitizer in the water droplets.

The sequence of reactions leading to photoinduced electron transfer, charge separation, and their degradation by the back electron transfer are summarized in eqs 1−4.

$$^1\text{EoEt}^- \xrightarrow{h\nu} {}^1\text{EoEt}^-* \quad (1)$$

$$^1\text{EoEt}^-* \xrightarrow{k_{isc}} {}^3\text{EoEt}^-* \quad (2)$$

$$^3\text{EoEt}^-* + \text{Fe(CN)}_6^{3-} \xrightarrow{k_q} {}^2\text{EoEt}^\bullet + \text{Fe(CN)}_6^{4-} \quad (3)$$

$$^2\text{EoEt}^\bullet + \text{Fe(CN)}_6^{4-} \xrightarrow{k_{rec}} {}^1\text{EoEt}^- + \text{Fe(CN)}_6^{3-} \quad (4)$$

In a previous study, it was demonstrated that ^{3}EoEt$^-$* is quenched by $Fe(CN)_6^{3-}$ in the water-in-oil microemulsion.[8] Photoexcitation of the chromophore in the microheterogeneous system that lacks the quencher results in the bleaching of the ground state, $\lambda = 539$ nm, and two broad absorbance peaks at 370 and 600 nm are observed. The latter two absorbance peaks are attributed[17] to the T−T absorption of ^{3}EoEt$^-$. In the presence of $Fe(CN)_6^{3-}$, an absorption band characteristic[18] of the oxidized chromophore ^{2}EoEt$^\bullet$ is observed at 460 nm. Thus, the characteristic absorbance features of the different species involved in the photoinduced redox reactions (^{3}EoEt$^-$*, $\lambda = 600$ nm; ^{2}EoEt$^\bullet$, $\lambda = 460$ nm; ^{1}EoEt$^-$, $\lambda = 520$ nm) enable us to elucidate the detailed mechanisms of photoinduced electron transfer, by following the transient behavior of the different species involved in the process.

To identify the basic functions of the water-in-oil microemulsion in charge separation, and the stabilization of the photoproducts against recombination, we followed the photoinduced electron-transfer process in the water-in-oil microemulsion using ethyl eosin, EoEt$^-$, or eosin, Eo^{2-}, as photosensitizers. The latter photosensitizer is confined in its ground state as well as in its oxidized state, $Eo^{\bullet-}$, to the water microdroplets, and thus charge separation is not expected to occur by the electron-transfer-induced hydrophobicity principle in the system that includes Eo^{2-} as a photosensitizer. Figure 1 (curve a) shows the transient absorbance of $Eo^{\bullet-}$ in the presence of $Fe(CN)_6^{3-}$ in the water-in-oil microemulsion system. The transient corresponds to the recombination of the photogenerated redox species, eq 5. The redox products decay within ca. 10 μs. Photoexcitation

$$^2\text{Eo}^{\bullet-} + \text{Fe(CN)}_6^{4-} \xrightarrow{k_{rec}} {}^1\text{Eo}^{2-} + \text{Fe(CN)}_6^{3-} \quad (5)$$

of the identical microheterogeneous system that includes EoEt$^-$ as a photosensitizer generates redox photoproducts that are extremely stable, Figure 1 (curve b). It can be seen that the electron-transfer products, eq 4, do not decay on a time scale of 150 μs. This result is consistent with the charge separation of the photoproducts by the electron-transfer-induced hydrophobicity principle, Scheme 1. The oxidized species ^{2}EoEt$^\bullet$ escapes from the aqueous microdroplet, and phase separation of the redox species leads to their stabilization against back electron transfer.

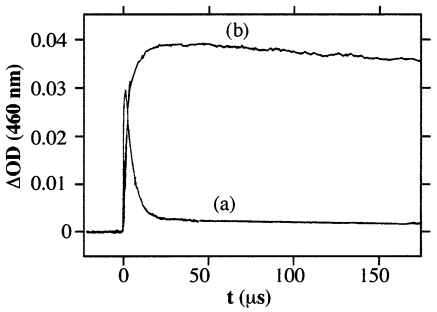

Figure 1. After-pulse evolution of the absorption band corresponding to the oxidized photosensitizer (either $^2Eo^{\bullet-}$ or ^{2}EoEt$^\bullet$), followed at $\lambda = 460$ nm, in the systems consisting of the following: (a) Eo^{2-} (10^{-5} M) and $Fe(CN)_6^{3-}$ (2.5×10^{-4} M) in reverse micelles ($w = 30$); (b) EoEt$^-$ (10^{-5} M) and $Fe(CN)_6^{3-}$ (2.5×10^{-4} M) in reverse micelles ($w = 30$).

The detailed quantitative analysis of the photoinduced electron-transfer and charge separation processes followed, with some modifications, models that were developed by Thomas,[19,20] Tachiya,[21,22] and others,[23] corresponding to the fluorescence quenching of chromophores in micellar systems. We assume a Poisson distribution of the quencher in the water droplets. Intermicellar exchange is neglected since it is slow compared to other processes involved in the electron transfer.[8] Self-quenching of the photosensitizer is discarded since the probability of finding two chromophore molecules in the same micellar-capped water droplet is negligible. The mathematical expressions describing the time-dependent concentrations of the triplet state, ^{3}EoEt$^-$*, the oxidized species, ^{2}EoEt$^\bullet$, and the concentration of the ground-state chromophore, ^{1}EoEt$^-$, are given by eqs 6−8, where λ is the quencher-to-micelle molar ratio, eq 9, $[^3\text{EoEt}^-*]_o$ is the concentration of the triplet state at time $t = 0$ (immediately upon excitation and intersystem crossing), θ_{esc} is the escape efficiency of the hydrophobic oxidized species, $\theta_{esc} = k_{esc}/(k_{rec} + k_{esc})$, and $k = k_{rec} + k_{esc}$.

$$[^3\text{EoEt}^-*](t) = [^3\text{EoEt}^-*]_o e^{-\lambda(1-e^{-kqt})} \quad (6)$$

$$[^2\text{EoEt}^\bullet](t) = [^3\text{EoEt}^-*]_o \sum_{n=1}^{\infty} \frac{\lambda^n e^{-\lambda}}{n!} \left\{ \theta_{esc} + \frac{nk_q}{nk_q - k} \left[(1-\theta_{esc}) e^{-kt} - \left(1 - \theta_{esc}\frac{k}{nk_q}\right) e^{-nk_q t} \right] \right\} \quad (7)$$

$$\Delta[^1\text{EoEt}^-](t) = -[^3\text{EoEt}^-*]_o \sum_{n=0}^{\infty} \frac{\lambda^n e^{-\lambda}}{n!} \left[\theta_{esc} + \frac{1-\theta_{esc}}{nk_q - k} (nk_q e^{-kt} - k e^{-nk_q t}) \right] \quad (8)$$

$$\lambda = [\text{Fe(CN)}_6^{3-}]/[m] \quad (9)$$

Figure 2 shows absorption transients of ^{3}EoEt$^-$* (followed at $\lambda = 600$ nm), (Part A), the oxidized photoproduct ^{2}EoEt$^\bullet$

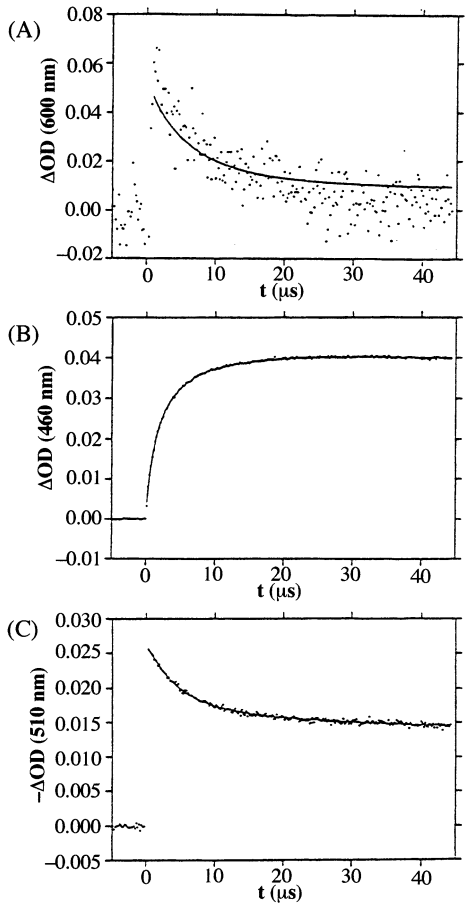

Figure 2. After-pulse evolution of the absorption transient corresponding to the following: (A) ^{3}EoEt$^-$*, followed at $\lambda = 600$ nm (fitting to eq 6 overlaid); (B) ^{2}EoEt$^\bullet$, followed at $\lambda = 460$ nm (fitting to eq 7 overlaid); (C) ^{1}EoEt$^-$ bleaching, followed at $\lambda = 510$ nm (fitting to eq 8 overlaid). The system consists of reverse micelles ($w = 30$) containing EoEt$^-$ (10^{-5} M) and $Fe(CN)_6^{3-}$ (2.5×10^{-4} M).

(followed at $\lambda = 460$ nm), (Part B), and the bleached ground-state chromophore, ^{1}EoEt$^-$ (followed at $\lambda = 510$ nm), (Part C), in the water-in-oil microemulsion system that includes $Fe(CN)_3^{3-}$, 2.5×10^{-4} M. The microemulsion system consists of a water-to-surfactant molar ratio corresponding to $w = [H_2O]/[AOT] = 30$, and the quencher-to-micelle molar concentration in the system was determined[8] to be $\lambda = 1.74$. Parts A−C of Figure 2 were fitted to the corresponding equations by the least-squares method, and the fitted curves are superimposed on the experimental transients. In this fitting process, it was enough to compute eqs 7 and 8 to the third degree ($n = 3$ included), since the probability of finding more than three quencher units in a microdroplet of a water-in-oil microemulsion exhibiting a $\lambda = 1.74$ value is less than 10%. For all of the fitting processes, λ was fixed, and the parameters $\epsilon d[^3\text{EoEt}^-\text{*}]_o$ (with ϵ corresponding to each of the species), k_q, θ_{esc}, and k were optimized. For the fitting shown in Figure 2C, corresponding to the recovery of the ground state, ^{1}EoEt$^-$, the contribution of the inherent decay of the unquenched triplet in the reverse micelles lacking the quenchers was taken into account. The fitting of the time-dependent evolution of the oxidized product, ^{2}EoEt$^\bullet$, Figure 2B (regression coefficient $R = 0.9993$), yields $\epsilon d[^3\text{EoEt}^-\text{*}]_o = 0.11$, $\theta_{esc} = 0.52$, $k_q = 1.7 \times 10^5$ s^{-1}, and $k = 1.1 \times 10^6$ s^{-1}. The fittings corresponding to the recovery of the ground-state chromophore ($R = 0.995$) and the decay of the triplet ($R = 0.80$; lower accuracy due to the lower signal sensitivity and the dependence on the inherent decay of the triplet) yield similar optimal values. The calculated rate constants for the intramolecular recombination and escape, cf. Scheme 1, are $k_{rec} = 5.3 \times 10^5$ s^{-1} and $k_{esc} = 5.7 \times 10^5$ s^{-1}, respectively.

The kinetic analysis reveals that, upon the excitation of ^{1}EoEt$^-$, and photoinduced electron transfer, the oxidized species formed, ^{2}EoEt$^\bullet$, is long-lived and does not decay on a microsecond time scale (cf. Figure 2B). The stability of the photogenerated redox species is attributed to their phase separation by means of hydrophobic/hydrophilic interactions. The phase-separated redox species recombine, however, at a millisecond time domain (see Figure 3(A), curve a). The transient decay of the oxidized species, ^{2}EoEt$^\bullet$, and the recovery of the bleached ground state, ^{1}EoEt$^-$, follow identical kinetics, implying that the two processes are interrelated. This is consistent with the fact that the decay of the oxidized species, ^{2}EoEt$^\bullet$, regenerates the ground state by the recombination process, eq 10. The derived value of the recombination rate constant is $k'_{rec} = 7.1 \times 10^2$ s^{-1}, which translates to a lifetime of ca. $\tau = 1.4$ ms for the phase-separated redox products.

$$^2\text{EoEt}^\bullet_{(oil)} + Fe(CN)_6^{4-}{}_{(aq)} \xrightarrow{k'_{rec}} {}^1\text{EoEt}^-_{(aq)} + Fe(CN)_6^{3-}{}_{(aq)} \quad (10)$$

The stabilization of the redox photoproducts against back electron transfer by means of their phase separation enables the design of a sequence of photoinduced electron-transfer reactions that could lead to enhanced quantum yields of a photochemical transformation under steady-state irradiation, Scheme 2. The photoinduced electron transfer occurring in the water droplet results in the transport of the oxidized photosensitizer to the oil phase. The electron donor localized in the hydrophobic phase reduces the transported oxidized species. This process yields the ground-state hydrophilic photosensitizer that is transferred back to the aqueous micropools. That is, the photosensitizer acts as an electron-transfer shuttle between the two phases. Accordingly, a hydrophobic donor, tributylamine, Bu_3N, is solubilized in the continuous hydrophobic phase of the water-in-oil microemulsion system. Extraction of the oxidized photoproduct, ^{2}EoEt$^\bullet$, to the oil phase by the electron-transfer-induced hydrophobicity principle is accompanied by the oxidation of the oil-phase-confined donor, eq 11. Upon oxidation of

$$^2\text{EoEt}^\bullet_{(oil)} + Bu_3N \xrightarrow{k_{red}} {}^1\text{EoEt}^-_{(aq)} + Bu_3N^{\bullet+} \quad (11)$$
$$\downarrow$$
oxidation products

tributylamine, the hydrophilic chromophore is regenerated, and is transferred back to the aqueous microdroplets. Thus, while the escape of the oxidized photoproduct to the oil phase competes with the intermicellar recombination process, the oxidation of the amine donor competes with the secondary recombination (k'_{rec}) between the oxidized product solubilized in the oil phase and the reduced species, $Fe(CN)_6^{4-}$, confined to the aqueous phase.

Laser flash photolysis experiments were applied to characterize the kinetics of the oxidation of tributylamine by ^{2}EoEt$^\bullet$ and the regeneration of the ground-state chromophore, ^{1}EoEt$^-$. Figure 3A shows the time-dependent decay of the oxidized product in the absence of Bu_3N (curve a) and upon increasing of the concentrations of Bu_3N (curves b−e). In the absence of Bu_3N, the decay of Bu_3N proceeds in the millisecond time domain, by processes corresponding to the secondary recombination of the oil-confined ^{2}EoEt$^\bullet$ with $Fe(CN)_6^{3-}$ solubilized in the aqueous droplets. Addition of Bu_3N significantly decreases the lifetime of ^{2}EoEt$^\bullet$. At high concentrations of Bu_3N, the

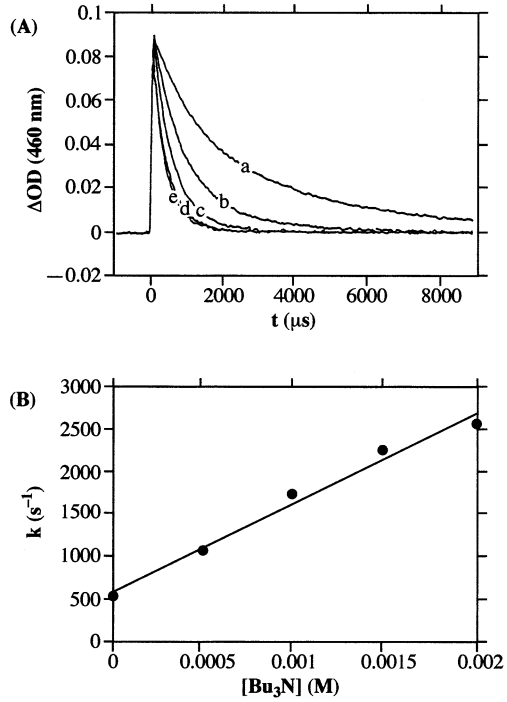

Figure 3. (A) Decay of the transient absorption of the oxidized state, ^{2}EoEt$^\bullet$, in the micellar systems ($w = 30$) that contain EoEt$^-$ (10^{-5} M), $Fe(CN)_6^{3-}$ (2.5×10^{-4} M), and Bu_3N—concentration range of 0 M (curve a) to 2.0×10^{-3} M (curve e) with differences of 0.5×10^{-3} M. (B) Decay rate of the oxidized state, ^{2}EoEt$^\bullet$ (derived from the exponential curves in part A), as a function of the donor, Bu_3N, concentration in the system.

lifetime of ^{2}EoEt$^\bullet$ is shortened to ca. one-fifth of the lifetime of the oxidized species in the absence of Bu_3N. An identical phenomenon is observed upon following the transients for the recovery of the bleached ground-state chromophore. That is, upon the increase of the concentration of Bu_3N, the recovery of the bleached species is faster. These results are consistent with the fact that the oxidation of the donor by the oxidized photoproduct in the oil phase, eq 11, regenerates the ground-state chromophore, ^{1}EoEt$^-$. All of the transient decay curves of ^{2}EoEt$^\bullet$ in the presence of Bu_3N, Figure 3A, follow mono-exponential kinetics. This suggests that ^{2}EoEt$^\bullet$ decays in a single phase and there is no distribution of decaying populations, characteristic of species dissolved in different micellar microenvironments. Figure 3B shows the plot of the rate of decay of ^{2}EoEt$^\bullet$ as a function of the concentrations of Bu_3N in the system. The rate constant for the decay of the oxidized species (k) is given by eq 12, where k'_{rec} is the secondary recombination rate

$$k = k'_{rec} + k_{red}[Bu_3N] \qquad (12)$$

constant and $k_{red}[Bu_3N]$ is the rate of reduction of ^{2}EoEt$^\bullet$ by Bu_3N, and hence depends on the donor concentration. The intercept of the linear plot shown in Figure 3B corresponds to k'_{rec}, while the slope of the line corresponds to k_{red}, $k_{red} = 1.1 \times 10^6$ $M^{-1}\cdot s^{-1}$.

The photoinduced electron transfer in the water-in-oil microemulsion system that includes the photosystem EoEt$^-$/$Fe(CN)_6^{3-}$/Bu_3N, and the function of the photosensitizer as an "electron shuttle" between the phases, were examined and characterized under steady-state irradiation. Two water-in-oil microemulsion systems were examined under continuous illumination. One photosystem includes eosin, Eo^{2-}, as a photosensitizer, and $Fe(CN)_6^{3-}$ and Bu_3N as the electron acceptor and electron donor, respectively. The photosensitizer in this

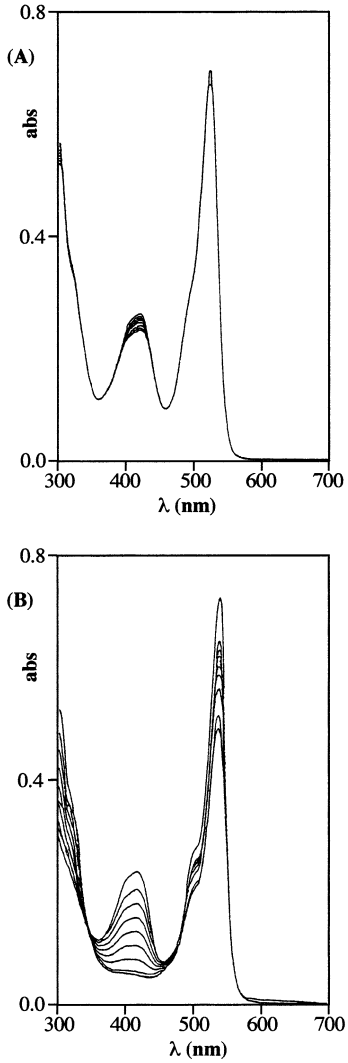

Figure 4. Absorption spectra at different time intervals of continuous irradiation ($\lambda > 495$ nm) (from $t = 0$ (upper curve) to $t = 10$ min (bottom curve)) of reverse micelle systems that contain (A) Eo^{2-} (10^{-5} M), $Fe(CN)_6^{3-}$ (2.5×10^{-4} M), and Bu_3N (10^{-3} M) and (B) EoEt$^-$ (10^{-5} M), $Fe(CN)_6^{3-}$ (2.5×10^{-4}), and Bu_3N (10^{-3} M).

system is hydrophilic in the ground state as well as in its oxidized state, $^2Eo^{-\bullet}$. Thus, this oxidized photoproduct is not expected to escape to the oil phase, and the electron-transfer quenching and recombination processes are expected to be confined to the aqueous microdroplets. The second photosystem includes the ^{1}EoEt$^-$ as a photosensitizer and $Fe(CN)_6^{3-}$ and Bu_3N as the electron-acceptor (quencher) and electron donor, respectively. Figure 4 shows the spectral changes of the water-in-oil microemulsions consisting of $^1Eo^{2-}$/$Fe(CN)_6^{3-}$/Bu_3N, Figure 4A, and ^{1}EoEt$^-$/$Fe(CN)_6^{3-}$/Bu_3N, Figure 4B, at time intervals of continuous irradiation, $\lambda > 495$ nm. Note that the photosystems are irradiated with filtered light that excludes the photoexcitation of $Fe(CN)_6^{3-}$ and side photoreactions.

In the photosystem that includes eosin, $^1Eo^{2-}$, as a photosensitizer, the electron acceptor is hardly reduced. In turn, in the presence of ^{1}EoEt$^-$, the electron acceptor, $Fe(CN)_6^{3-}$, is rapidly reduced, as evidenced by the fast depletion of its characteristic absorbance, $\lambda = 410$ nm. Figure 5 shows the effectiveness of photoinduced reduction of $Fe(CN)_6^{3-}$ (molar concentration or percentage of reduction) in the photosystems. In the microheterogeneous assembly that includes ^{1}EoEt$^-$ as a photosensitizer, the light-induced reduction of the electron acceptor proceeds almost linearly, and after 7 min ca. 95% of

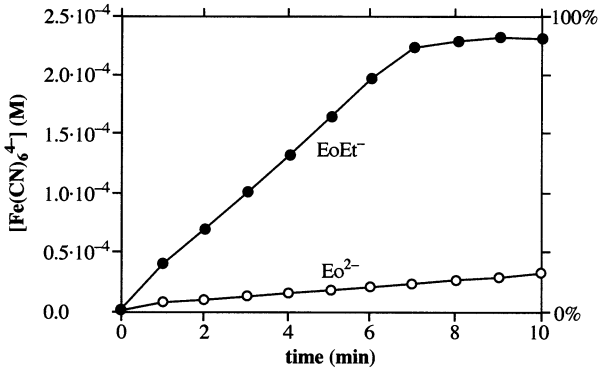

Figure 5. Conversion of $Fe(CN)_6^{3-}$ to $Fe(CN)_6^{4-}$ (molar concentration or percentage of reduction) as a function of time in the reverse micellar systems presented in Figure 4 (Eo^{2-} or $EoEt^{-2}$ act as photosensitizers).

$Fe(CN)_6^{3-}$ are reduced. On the other hand, in the water-in-oil microemulsion system that includes Eo^{2-} as a photosensitizer, only 5% of the electron acceptor are reduced within this time interval of illumination. Thus, the effectiveness of photoreduction of $Fe(CN)_6^{3-}$ by $^1EoEt^-$ is 20-fold higher than the reduction yield by the dianionic photosensitizer, Eo^{2-}. This result is attributed to the electron-transfer-induced hydrophobicity property of the oxidized product in the system that includes $^1EoEt^-$ as a photosensitizer. The escape of the oxidized photoproduct, $^2EoEt^{\bullet}$, following the electron transfer, results in the phase separation of the photoproducts and their stabilization against back electron transfer. The long-lived $^2EoEt^{\bullet}$ allows the effective subsequent oxidation of Bu_3N and the regeneration of the photosensitizer. Thus, the photosensitizer $^1EoEt^-$ acts as an electron-transfer shuttle that mediates electron transfer across the water−oil boundary of the water-in-oil microemulsion, leading to the light-induced reduction of $Fe(CN)_6^{3-}$ by Bu_3N. In the photosystem that includes Eo^{2-} as a photosensitizer, the oxidized photosensitizer is hydrophilic and is not extracted to the oil phase. As a result, the photogenerated redox species recombines rapidly in the aqueous microdroplets. The confinement of the oxidized chromophore to the aqueous microenvironment prevents the efficient oxidation of Bu_3N, and consequently, most of the redox intermediates are degraded by the intermicellar recombination. The inefficient reduction of $Fe(CN)_6^{3-}$ in the photosystem that includes the Eo^{2-} photosensitizer is attributed to the partial assembly of Bu_3N at the oil−water boundary of the micellar system that leads to the partial scavenging of $^2Eo^{\bullet-}$ solubilized in the water microdroplets. It should be noted that, in the $^1EoEt^-/Fe(CN)_6^{3-}/Bu_3N$ photosystem, bleaching of the photosensitizer is observed after ca. 95% of the electron acceptor is reduced to $Fe(CN)_6^{4-}$. The bleaching process is evident by the degradation of the absorbance band, $\lambda = 514$ nm, characteristic of the chromophore. This bleaching process is attributed to the irreversible reductive quenching of $^3EoEt^{-*}$ by $Fe(CN)_6^{4-}$. Thus, the accumulation of $Fe(CN)_6^{4-}$ in the system results in the degradation of the light-active component.

The quantum yield for the reduction of $Fe(CN)_6^{3-}$ in the $^1EoEt^-/Fe(CN)_6^{3-}/Bu_3N$ water-in-oil microemulsion system was estimated to be $\phi = 0.04$. Theoretically, the quantum yield of the photoprocess is the product of the triplet quantum yield, ϕ_T, and the effectiveness of the other processes leading to the product, as expressed by eq 13, where ϕ_T is the triplet yield, $\phi_T = 0.76$, the term $(1 - e^{-\lambda})$ is the fraction of reverse micelles that includes at least one quencher unit, θ_{esc} is the escape yield to the oil phase, $\theta_{esc} = 0.52$, θ_{red} is the yield for the reduction of the oxidized species by the donor, $\theta_{red} = k_{red}[Bu_3N]/(k'_{rec} + k_{red}[Bu_3N])$, $\theta_{red} = 0.65$, and θ_{ox} is the yield for the irreversible degradation of the oxidized donor, $Bu_3N^{\bullet+}$, a process that competes with the thermodynamically possible recombination of $Bu_3N^{\bullet+}$ with $Fe(CN)_6^{4-}$. Taking into account the experimental quantum yield for the photoreduction of $Fe(CN)_6^{3-}$, we estimate that $\theta_{ox} = 0.19$. Thus, provided an improved electron donor, which instantaneously decomposes upon oxidation, could be selected, the maximum quantum yield for the reduction of $Fe(CN)_6^{3-}$ in the microheterogeneous system could be $\phi = 0.21$.

$$\phi = \phi_T(1 - e^{-\lambda})\theta_{esc}\theta_{red}\theta_{ox} \quad (13)$$

Conclusions

The present study addressed a novel approach to the control of photoinduced electron-transfer processes in microheterogeneous water-in-oil microemulsion systems. We have described the use of the electron-transfer-induced hydrophobicity principle to stabilize photoproducts against the back-electron-transfer process. That is, by the application of the monoanionic dye, $^1EoEt^-$, as a photosensitizer and $Fe(CN)_6^{3-}$ as an electron acceptor, effective electron transfer occurred in the aqueous microdroplets. Escape of the photogenerated hydrophobic oxidized product, $^2EoEt^{\bullet}$, to the oil phase led to the phase separation of the redox products and to their stabilization against back electron transfer. The oxidized photoproduct was then coupled to the secondary oxidation of tributylamine, Bu_3N, in the oil phase. This process regenerated the hydrophilic photosensitizer, $^1EoEt^-$, and led to its re-extraction to the aqueous phase. Thus, we demonstrated the application of an electron shuttle photosensitizer that mediated electron transfer through the water−oil interface of the microheterogeneous system. The phase separation of the photoproducts and the mediated electron transfer led to an efficient reduction of $Fe(CN)_6^{3-}$ by Bu_3N, $\phi = 0.04$. The incorporation of secondary catalysts into the aqueous and oil phases is anticipated to enable subsequent effective photosynthetic transformations.

Acknowledgment. This research was supported by the Volkswagen Stiftung, Germany.

References and Notes

(1) (a) Willner, I.; Willner, B. *Top. Curr. Chem.* **1991**, *159*, 153. (b) Fox. M. A. *Top. Curr. Chem.* **1991**, *159*, 67.

(2) (a) Pileni, M. P.; Brochette, P.; Pigeonniere, B. L. *NATO Adv. Sci. Ser. C* **1986**, *165*, 253. (b) Willner, I.; Ford, W. E.; Otvos, J. W.; Calvin, M. *Nature* **1979**, *280*, 830.

(3) Fendler, J. H. *Chem. Rev.* **1987**, *87*, 877.

(4) Joselevich, E.; Willner, I. *J. Phys. Chem.* **1994**, *98*, 7628.

(5) (a) Mandler, D.; Degani, Y.; Willner, I. *J. Phys. Chem.* **1984**, *88*, 4366. (b) Ulrich, T.; Steiner, U. E. *Chem. Phys. Lett.* **1984**, *112*, 365. (c) Ulrich, T.; Steiner, U. E.; Schlenker, W. *Tetrahedron* **1986**, *42*, 6131.

(6) Luisi, P. L.; Magid, L. *Crit. Rev. Biochem.* **1986**, *20*, 409.

(7) Verhaert, R. M. D.; Shaafsma, T. J.; Laane, C.; Hilhorst, R.; Veeger, C. *Photochem. Photobiol.* **1989**, *49*, 209.

(8) Joselevich, E.; Willner, I. *J. Phys. Chem.* **1995**, *99*, 6903.

(9) (a) Valdes-Aguilera, O.; Neckers, D. C. *Acc. Chem. Res.* **1989**, *22*, 171. (b) Flamigni, L. *J. Phys. Chem.* **1992**, *96*, 3331. (c) Kashe, V.; Lindqvist, L. *J. Phys. Chem.* **1964**, *68*, 817.

(10) (a) Nemoto, N.; Kokubun, H.; Koizumi, M. *Bull. Chem. Soc. Jpn.* **1969**, *42*, 1223. (b) Rodgers, M. A. J. *J. Phys. Chem.* **1981**, *85*, 3372. (c) Seret, A.; Gandin, E.; Van de Vorst, A. *J. Photochem.* **1987**, *38*, 145.

(11) (a) Lee, P. C. C.; Rodgers, M. A. J. *Photochem. Photobiol.* **1987**, *45*, 79. (b) Vintgens, V.; Scaiano, J. C.; Linden, S. M.; Neckers, D. C. *J. Org. Chem.* **1989**, *54*, 5242. (c) Murasecco-Suardi, P.; Gassmann, E.; Braun, A. M.; Oliveros, E. *Helv. Chim. Acta* **1987**, *70*, 1760.

(12) (a) Willner, I.; Eichen, Y.; Joselevich, E.; Frank, A. J. *J. Phys. Chem.* **1990**, *94*, 3092. (b) Willner, I.; Eichen, Y.; Joselevich, E. *J. Phys. Chem.* **1992**, *96*, 6061.

(13) Moser, J.; Grätzel, M. *J. Am. Chem. Soc.* **1984**, *106*, 6557.

(14) Kamat, P. V.; Fox, M. A. *Chem. Phys. Lett.* **1983**, *102*, 379.

(15) Schwarz, G. *Sci. Ind. Photogr.* **1937**, *2*, 97.

(16) (a) Willner, I.; Zahavy, E. *Angew. Chem., Int. Ed. Engl.* **1994**, *33*, 581. (b) Willner, I.; Zahavy, E.; Heleg-Shabtai, V. *J. Am. Chem. Soc.* **1995**, *117*, 542.

(17) For comparison, triplet eosin exhibits a lifetime of 95 μs, $\phi_T = 0.75$, and a T−T absorbance at $\lambda = 600$ nm, cf. Moser, J.; Grätzel, M. *J. Am. Chem. Soc.* **1984**, *106*, 6557.

(18) For a detailed characterization of photoinduced electron transfer between eosin and $Fe(CN)_6^{3-}$ in water, see: Kashe, V.; Lindqvist, L. *Photochem. Photobiol.* **1965**, *4*, 928.

(19) Atik, S. S.; Thomas, J. K. *J. Am. Chem. Soc.* **1981**, *103*, 3543.

(20) Infelta, P.; Grätzel, M.; Thomas, J. K. *J. Phys. Chem.* **1974**, *78*, 190.

(21) (a) Tachiya, M. *J. Phys. Chem.* **1983**, *87*, 5282. (b) Tachiya, M. *Chem. Phys. Lett.* **1975**, *33*, 289.

(22) Tachiya, M. In *Kinetics of Nonhomogeneous Proceses;* Freeman, G. R., Ed.; John Wiley & Sons: New York, 1987; p 575.

(23) Lianos, P.; Malliaris, A. *Isr. J. Chem.* **1991**, *31*, 177.